Appl Phys A (2009) 94: 871–878
DOI 10.1007/s00339-008-5018-9

Applied Physics A
Materials Science & Processing

Dating study of two rock crystal carvings by surface microtopography and by ion beam analyses of hydrogen

T. Calligaro · Y. Coquinot · I. Reiche · J. Castaing · J. Salomon · G. Ferrand · Y. Le Fur

Received: 30 April 2008 / Accepted: 24 November 2008 / Published online: 18 December 2008

Abstract Two artefacts made of rock crystal (quartz) from the collection of the *Musée du quai Branly* in Paris, France, a skull approximately half of the size of a real cranium and a smaller anthropomorphic head, purportedly attributed to pre-Columbian Mesoamerican cultures, were studied to assess their authenticity. The surface of the artefacts were examined by means of optical microscopy and scanning electron microscopy (SEM) and were analyzed nondestructively by ERDA (Elastic Recoil Detection Analysis), an ion beam analytical method that can measure hydrogen concentration profiles in depth. Optical and SEM imaging of tool marks indicates that the skull has been cut from a rock crystal block using machine lapidary techniques unavailable to pre-Columbian artisans, whereas the anthropomorphic head has more likely been carved and polished with manual techniques comparable to ancient ones. Hydrogen depth profiles in the first micron below the surface of the artefacts have been measured by ERDA with a 3-MeV He beam in a controlled helium atmosphere. Recently the progressive penetration of water at the surface of a quartz sample exposed to the natural environment has been proposed as a dating method (labeled quartz hydration dating or QHD) applicable to archaeological artefacts made of this material. The shallower penetration of H clearly indicates that the rock crystal skull was manufactured more recently than the reference quartz sample cut in 1740. As for the anthropomorphic head, the deep penetration profiles indicate an older artefact. Thus the converging micro-topographical examinations and hydrogen profiles of the samples surfaces indicate that the skull is probably not a pre-Columbian artefact but has been carved in the 18th or 19th century. The anthropomorphic head, on the other hand, could have been carved in the pre-Columbian period. In addition, the ERDA method carried out with an external beam presented here provides a new and simple approach for the nondestructive authentication of quartz-based archaeological artefacts by QHD.

PACS 61.72.Ww · 81.05.Je · 81.70.Jb · 82.80.Yc

1 Introduction

Many rock crystal skulls carved before the middle of the 20th century are claimed to be artefacts manufactured by pre-Columbian Mesoamerican cultures, although none has been retrieved from a documented archaeological excavation. Among the around ten large quartz skulls that appeared before 1930, three famous ones are conserved in museums, namely the *British museum* in London, the *Smithsonian Institution* in Washington, and the *Musée du quai Branly* in Paris, the others being in private collections. Whereas Mesoamerican art has numerous examples of skulls made of stone, such quartz skulls have little stylistic or technical relationship with these genuine archaeological artefacts. Jane Walsh, anthropologist at the *Smithsonian Institution*, who has long been investigating these skulls from both bibliographic and scientific points of view, has cast serious doubts

T. Calligaro (✉) · Y. Coquinot · I. Reiche · J. Castaing · J. Salomon
Centre de recherche et de restauration des musées de France—C2RMF, CNRS UMR171, Palais du Louvre, 75001 Paris, France
e-mail: thomas.calligaro@culture.gouv.fr

G. Ferrand
Ecole nationale supérieure des mines de Paris, 75006 Paris, France

Y. Le Fur
Musée du quai Branly, 75007 Paris, France

on the pre-Columbian origin of some of them [1]. Today institutions like the *British Museum* exhibits skulls as examples of fakes, while other institutions still present them as the genuine pre-Colombian artefacts.

In a recent paper [2] on the crystal skulls of the *British Museum* and of the *Smithsonian Institution*, Sax and co-workers mention that an initial examination in the 1960s of the surface of the London skull showed carving marks attributed to rotary tools unavailable to pre-Columbian artisans. In their extensive study, the marks and material left from the lapidary work on the two skulls were compared to a genuine Mixtec (1500–1521 A.D. period, A.D. = Anno Domini) quartz goblet. Specific striations observed on the skulls were attributed to the use of modern rotary equipment, whereas the goblet showed only marks attributed to manual carving with simple nonrotating tools. In addition, fluid and mineral inclusions observed in the quartz of the skull of the *British Museum* were interpreted as an argument for an Alpine or Brazilian provenance of the quartz, rather than a Mexican origin. It was concluded that these objects were probably crafted in the 19th century.

Carving techniques used by Chinese and Egyptian craftsmen have been extensively studied, but little is known about the ancient lapidary techniques used by pre-Columbian artisans to work quartz, jade, or other hard materials. The numerous quartz artefacts found in pre-Columbian excavations is evidence that these people were working such a hard material [3], but the nature of the tools and of the abrasive substances they used are still investigated [4]. It is however agreed that tools rotating about an axis such as the wheel-cutting were not employed in pre-Columbian technology [2].

The two quartz artefacts studied here (Fig. 1), the skull ref. 71.1878.1.57 approx. half size of a real cranium and a smaller anthropomorphic head ref. 71.1878.1.217.Am with

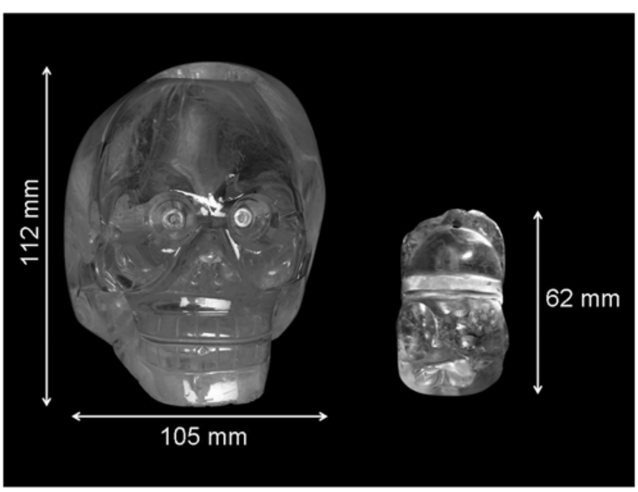

Fig. 1 *Left*, the rock crystal skull ref. 71.1878.1.57 labeled SK; *right*, the anthropomorphic head ref. 71.1878.1.217.Am labeled SP

the mention "Pachuca, Hidalgo" were donated by the French explorer and ethnographer Alphonse Pinart in 1878 to the *Musée d'Ethnographie du Trocadéro* in Paris, later renamed *Musée de l'Homme*. The two carvings are now conserved, with a large part of the collections of the *Musée de l'Homme*, in the recently opened *Musée du quai Branly* in Paris. Pinart had bought most of his collection in 1875 in Paris, including the two objects under study here, from Eugène Boban-Duvergé, a controversial French antique dealer resident in Mexico during the reign of the emperor Maximilian [5]. Boban probably acquired the large skull after his return to France in 1870 and exhibited it in 1875 at the 1st meeting of the International Congress of Americanists in Nancy [6], just prior the time when Pinart bought it. Indeed, the skull is not reported on any earlier list or catalogue from Boban, and it was not possible to trace back its history before that period. On the other hand, the small anthropomorphic head appears earlier, its presence being attested in the inventory of Boban's first collections established in Mexico.

2 Examination

2.1 Sample description and methodology

The quartz nature of both samples was confirmed by recording the Raman spectrum with a Horiba Jobin Yvon Infinity Raman micro-spectrometer with a 532 nm green laser delivering a power of less than 4 mW on the sample. The skull (sample labeled SK) has dimensions L 145 × W 105 × H 112 mm (Fig. 1) and weighs 2.54 kg. A slightly bi-conical 20 mm diameter hole has been vertically drilled in its center. A comparably pierced although smaller skull (ca. H 70 mm) from a private collection was used as the base for a crucifix [7], sample SK could have had a similar function. The anthropomorphic pre-Columbian head (sample labeled SP), smaller than SK, measures L27 × W38 × H 62 mm (Fig. 1) and weighs 0.082 kg. The quartz is transparent, but iron oxides, low magnesium content calcite, and other impurities partially cover the back of the artefact.

Surfaces of both artefacts were first examined for tool marks using a binocular microscope with magnification up to 40×. Surface replicas from selected areas were taken with a silicone resin model RTV 181 and coated with gold for SEM (PHILIPS XL30 ESEM) examination with secondary electron imaging at magnifications of 20× to 100×. This method is derived from the technique introduced by Sax for surface microscopic examination of quartz carvings [8]. The replica method avoids the application of a conductive coating to the artefact and its exposure to high vacuum in the SEM, which in any event would not be feasible for sample SK due to its large size. Moreover, this method permits the examination of deeply carved and poorly accessible areas which are difficult to smooth and polish (and are unlikely to have been affected by restoration) and therefore might better preserve the original tool marks. The marks on replicas have been mapped using an optical 3-D profilometer model Micromeasure from STIL company [9].

Three areas of sample SK surface have been selected by binocular microscope observations to be molded for replicas: the orbits, the longitudinal grooves delimiting teeth, and the polished surface on the top of the skull. Note that replicas record carved features negatively: the features that appear as protrusions in the SEM images of the replicas represent depressions, hollows, or cavities in the artefacts.

2.2 Results and discussion

Observation by binocular microscopy showed numerous original tool marks, mainly in the bottom and on the internal surfaces of the eye orbit but also in the engraved lines delimiting the teeth. While it appears easy to distinguish patterns made by ancient tools from modern ones, it is difficult to definitely ascribe surface features to a given technique. Scores left by pre-Columbian tools are expected to appear uneven and to be nonparallel. Modern stone-carving and polishing tools (after the 19th century) leave very regular, uniform, and parallel marks, while the abrasives used for manual crafting tend to move around the tool when applied to the surface of the artefact and their movement is randomly oriented. On the other hand, modern abrasives that are permanently bonded to engraving and polishing metallic tools leave neat, even, and parallel grooves and scratches.

Different surface features have been observed on the surface of both artefacts and were interpreted in terms of four lapidary techniques: coring, drilling, wheel-cutting, and polishing. From tool marks on the eyes and teeth from sample SK, three basic techniques of engraving have been identified. These are coring (circular feature), drilling (circular feature), and wheel-cutting (curvilinear features). Each technique can be recognized by a set of criteria: surface texture, shape (plan view), and depth (side view). The morphology of surrounding surfaces was also noted; e.g., whether the local surface had been worked to a convex, concave, or flat shape.

At 40×, the surface texture on sample SK shows a faint parallel longitudinal grooving corresponding to fine polishing. The bottom surface of engraved lines delimiting the teeth is marked by parallel and continuous longitudinal striations (Fig. 2a). As can be seen in the profile of the replica recorded with the 3-D profilometer (Fig. 2b), its longitudinal profile is almost straight and slightly concave at the end. This type of profile could not be interpreted as a rotating wheel mark as it was the case for similar marks on the *British museum* skull [2], but it rather seems to be as a mark left by filing. In the bottom of the eye‘s orbit, a deep and regular, 500-μm-width ring-shaped groove at the periphery and conchoidal fractures in the center were observed (Fig. 2c), probably due to coring. The very narrow and constant width of the annular groove suggests the use of a modern trepan. Moreover, very regular, circular, and parallel marks observed on the internal surface (Fig. 2d) and in the bottom of the orbits could have been induced by drilling with a rotary tool, and the orbit shape indicates the use of one or two conical tools (Fig. 2e). The high regularity of the shape suggests also that the cavity was drilled using a rotary machine with a fixed axis oriented perpendicular to the surface. The conical orbits show also two annular rings, one in the middle and the other on the bottom, suggesting that they have been drilled in two sequences. These rings are due to the accumulation of ground quartz and possibly abrasive powder under the tool head. Wheels and other rotary tools are not known in pre-Columbian cultures. The marks observed on sample SK do not seem to have been produced by the rudimentary stone, bone, wood, or possibly metal tools combined with abrasive powders available to pre-Columbian lapidaries. Sample SK has most likely been carved with relatively modern lapidary equipment, which were unavailable to pre-Columbian Mesoamerican craftsmen.

On the other hand, the surface of the anthropomorphic head SP displays grooves with various depths and different orientations (Fig. 2f). The variable width of the marks suggests the use of abrasive powders containing grains of different sizes [8]. These observations, similar to those by Sax and co-workers on the Mixtec goblet (Fig. 3b in Ref. [2]), suggest the use of rudimentary tools and techniques.

3 Hydrogen profile by ion beam analysis

3.1 Principle of quartz hydration dating (QHD)

The slow uptake of elements from the environment by the freshly cut surface of mineral artefacts has been proposed as a marker to date archaeological objects made of obsidian [10], flint [11], and more recently rock crystal (quartz). The principle is to measure the time-dependent penetration depth of an external element to provide information on the date of manufacture of the object. Ericson [12] has proposed to use the penetration of water as a dating method for quartz, labeled QHD for quartz hydration dating, and suggested its applicability to artefacts in the range extending from 100 to 100 000 years. With the assumption of diffusion in a semi-infinite medium with a concentration-independent diffusion coefficient, the hydrogen concentration profile $H(x,t)$ at a depth x in the crystal after time t follows Fick's law [13]

$$H(x,t) = \left(H(0,t) - c_i\right) \cdot \operatorname{erfc}\left\{x/2(Dt)^{-1/2}\right\} + c_i, \qquad (1)$$

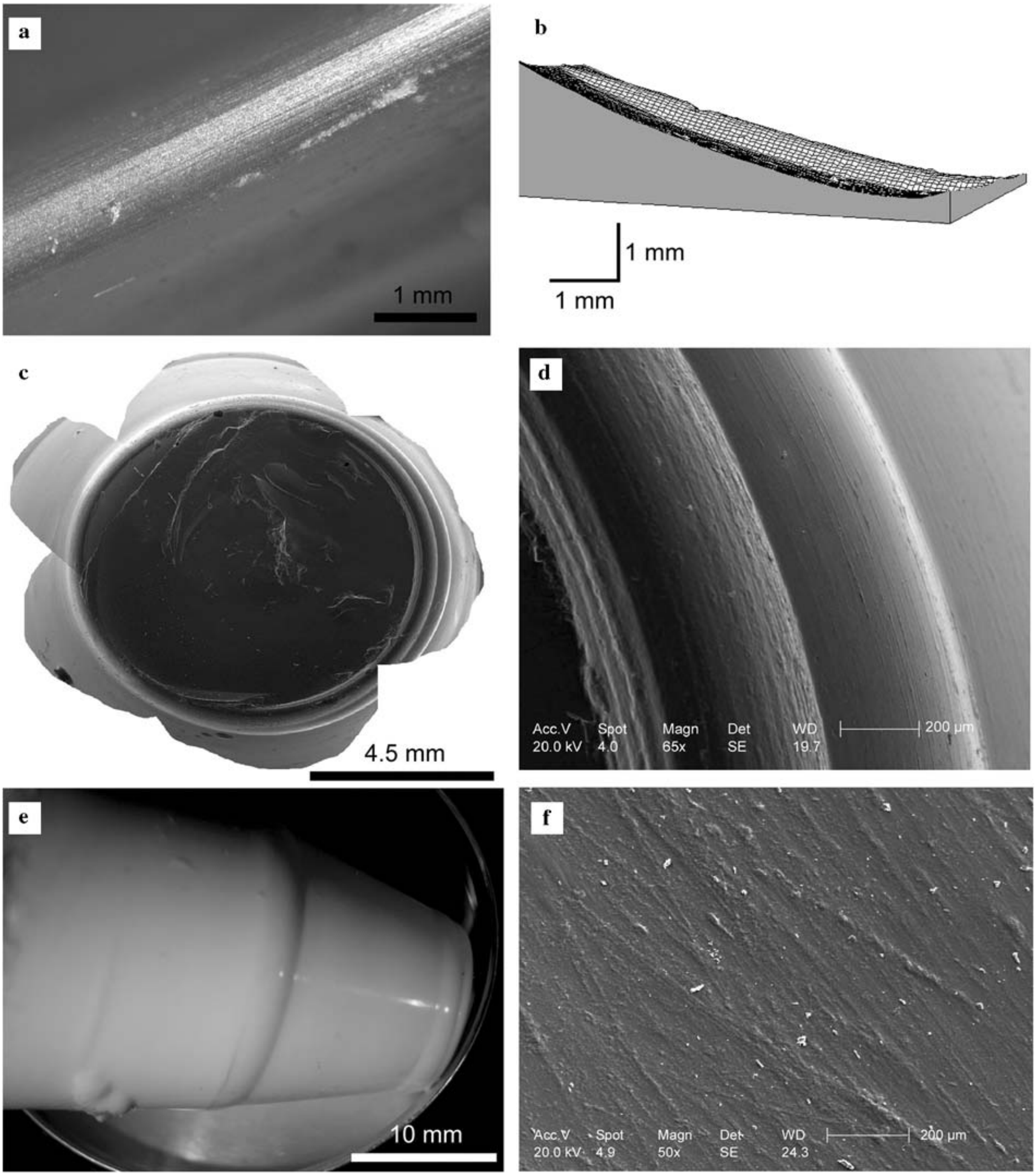

Fig. 2 **a** Optical image of the parallel and continuous grooves on the internal surface of a engraved line delimiting the teeth. **b** Longitudinal profile of the groove delimiting teeth obtained by 3-D optical profilometer on a replica (appearing as a protrusion instead of groove). The curvature is not compatible with machining with a rotation wheel. **c** SEM image of the bottom of the right eye orbit showing ring-shaped grooves attributed to coring techniques and the conchoidal fracture resulting from breaking the quartz core. **d** SEM image of circular and parallel grooves on the wall of the right eye orbit, revealing the use of rotary drilling technique. **e** Optical image of the orbit replica showing the conical shape of the tools used to machine the eye orbit and the presence of two annular rings. **f** SEM image of the surface of the anthropomorphic head showing striations with various depths and random orientations

where erfc is the complementary error function, D the diffusion coefficient, and c_i the initial bulk hydrogen concentration in quartz. It must be noted that the penetration depth is proportional to the square root of t, and thus its progression tends to slow down with increasing age. For historic ages, H diffusion profiles in quartz at room temperature extend to less than one micrometer. In this weathering process, the source of water is the natural environment (air, soil), and the diffusivity was found to be independent of the surface concentration $H(0,t)$ [14], the layer of *ca.* 10^{16} mol/cm^2 of H_2O naturally adsorbed on the surface of an artefact placed in air being sufficient to encourage H diffusion. The hydration level, even close to the surface, is relatively low (less than a few % at of H), and thus for calculations, the diffused layer could be considered as pure quartz. From measurements on artificially aged synthetic quartz crystals below 200°C and archaeological samples, Dersch and co-workers [15, 17] have found that the diffusion coefficient D depends only upon three parameters: temperature T, crystal orientation α, and initial bulk hydrogen content c_i. The temperature dependence of D follows the Arrhenius law

$$D(T) \sim \exp(-E_a/RT). \tag{2}$$

Here, T is in Kelvin, E_a is the activation energy (57 kJ/mole for quartz), and R the gas constant $= 8.31\ \mathrm{J\,mol^{-1}\,K^{-1}}$. Regarding the influence of crystal orientation, natural quartz is trigonal with the symmetry axis called c along [0001], and the diffusion process appeared to depend exponentially on the angle α between the surface normal and [0001]. The sharply peaked distribution of D at $\alpha = 0°$ (50× the value measured at $\alpha = 90°$) was attributed to the presence of open diffusion channels in that direction, and as a consequence, the orientation of the c-axis of the samples has to be precisely determined. This empirical dependency remains surprising, as simple physical considerations would rather suggest a dependency upon $\cos\alpha$. The last parameter is the bulk hydrogen concentration c_i. During its hydrothermal growth, quartz traps a homogenous bulk hydrogen content c_i up to a fraction of at.% and D was found to be proportional to this content. This linear dependence has been experimentally studied [14] in a limited range of c_i, from 0.001 to 0.062 at.% H. Note that the hydrogen profiles following (1) correspond to the solution of the equation of diffusion in the case of a constant diffusion coefficient. A concentration-dependent diffusion model would generate profile shapes quite different [16] from those observed experimentally and derived from (1). The c_i value might rather be considered as a link to the density of defects in the crystal surface layer (impurities, dislocations, twins, etc.) modulating the diffusion. The accurate measurement of this low level of hydrogen is necessary for QHD.

To summarize, the following semi-empirical formula [17] has been proposed to account for the dependence of the D coefficient upon the three parameters T, α, c_i:

$$D(T,\alpha,c_i) = 8.610^{-12} c_i \exp(-E_a/RT) \times \exp(-0.044\alpha + 0.03) \tag{3}$$

with c_i in at. ppm, T in Kelvin, α in degrees, and D in $\mathrm{cm^2\,s^{-1}}$.

3.2 Experimental

In the previous works, the hydrogen depth profiles have been determined by means of an analytical method based on a resonant nuclear reaction [18] between a beam of ^{15}N ions and the hydrogen in the target, namely the ^{1}H(^{15}N, $\alpha\gamma$)^{12}C reaction occurring at 6.385 MeV with detection of the emitted prompt γ-ray of 4.44 MeV. When ^{15}N ions have exactly the energy of the resonance, the surface of the sample is probed. By increasing progressively the ^{15}N ion energy up to 14 MeV, the depth at which the nuclear reaction occurs is displaced from the surface towards the inner of the sample, making it possible to record H profiles in quartz up to 2.5 μm [15].

The present results were obtained by an alternative method, namely elastic recoil detection analysis [19] (ERDA). Indeed, the NRA method employed previously cannot be performed with our accelerator, its maximum energy being too low. The principle of ERDA is to bombard the sample at a grazing angle (15°) with ions heavier than protons (usually He ions) and to detect the hydrogen scattered out of target in the forward direction. The energy of recoiled hydrogen ions depends on the depth where the scattering occurred, and thus their energy spectrum yields a concentration depth profile. The experiment was carried out with 3-MeV ^{4}He^{++} ions in the external microbeam line of the C2RMF accelerator [20]. The samples were placed in a closed vessel filled with an atmosphere of pure helium gas. This set-up and initial results have been described elsewhere [21]. The analysis is performed in standard geometry (Fig. 3), the beam impinging at 15° relative to the sample surface and the expelled hydrogen ions detected at a 15° exit angle, i.e., 30° diffusion angle, with a 300-mm^2

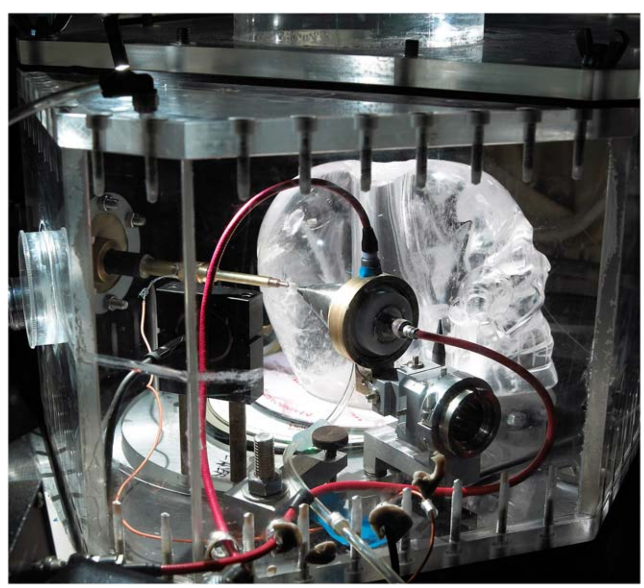

Fig. 3 Sample SK positioned in the ERDA set-up

100-µm-thick planar Si detector screened with a 13-µm Kapton foil to stop elastically scattered He ions. The detector is located 80 mm from the target, and a rectangular diaphragm of 5 × 1 mm^2 is used to reduce uncertainty in the kinetic factor. Under these conditions, the maximum probed depth in quartz is of the order of one micrometer. A key feature of the external ERDA set-up is the use of two 100-nm-thick Si_3N_4 membranes that isolate the beam line and detector housing (which are under vacuum) from the surrounding helium atmosphere. The incident He ions and forward scattered hydrogen ions only travel a few millimeters in the helium gas before and after the beam impact, minimizing the energy straggling. Spectra were acquired in runs of 20 to 40 minutes and a beam intensity of ca. 10 nA, with a fixed dose of 20 µC. The raw ERDA spectra (counts vs. energy) were converted to diffusion profiles (H concentration vs. depth) with a procedure based on a simulation using the SIMNRA program [22] with the non-Rutherford diffusion cross section of He ions on H from Baglin et al. [23]. The set-up was calibrated against a muscovite mica sample $KAl_2(AlSi_3O_{10})(OH)_2$ containing 10% at of H and checked on a synthetic quartz implanted with 5×10^{16} at H cm^{-2} at 40 keV.

An advantage of the ERDA method is that it provides the entire H depth profile in a single run, whereas the ^{15}N method is more complex and time-consuming as it needs a γ-ray spectrum for each point of the profile. Moreover, the irradiation with a 10-µC beam dose of He ions required to obtain a full H profile by ERDA compared to the ca. 200 µC of ^{15}N ions needed with the nuclear method [24] reduces the risk of alteration of the H content during the experiment. On the other hand, due to its grazing geometry, ERDA can only be applied on a sample having a flat and polished surface. This constraint is however partly overcome using a microbeam since the analyzed spot is less than 0.5 × 0.1 mm^2 and can be considered as a flat zone. Finally the consistency of ^{15}N, ERDA, and SIMS methods for the determination of H depth profiles has been demonstrated [25].

3.3 Results and discussion

In addition to sample SK and sample SP, we have analyzed a third sample, which is a fragment of a pendant of a chandelier manufactured for the Sanssouci castle in Potsdam, Germany (sample labeled SS). The latter, precisely dated to 1740 A.D. and already analyzed in a previous work [25] was used as a reference in this study. Sample SS presents a small but clear surface that could be oriented in the ERDA geometry. Examination of samples with crossed-polars permitted to tell that the analyzed areas of the three samples SS, SP, and SK were oriented at $\alpha = 75°$, 90°, and 90°, respectively, with an error of ca. 5°. Figure 3 illustrates the positioning of sample SK in the ERDA set-up, and Fig. 4 gives the spectra recorded on the three samples (several spectra for each sample obtained on adjacent regions). The ERDA spectra exhibit specific features: (a) a marked peak at the surface, corresponding to the overlap of the water layer at the surface and the first part of the diffusion profile, (b) a decay in the 600–800 keV region with markedly different slopes for the two archaeological artefacts, sample SK having a steeper slope than sample SP, and an intermediate slope for reference sample SS, and (c) a low-energy plateau which was interpreted as the initial bulk hydrogen concentration c_i. Quantitative hydrogen diffusion profiles were derived from these raw data (Figs. 5, 6, and 7 for sample SS, SP, and SK, respectively), the data points being fitted with (1) using the Statistica software [26]. Table 1 shows that the values obtained, $H(0,t)$ surface concentrations and D·t products for

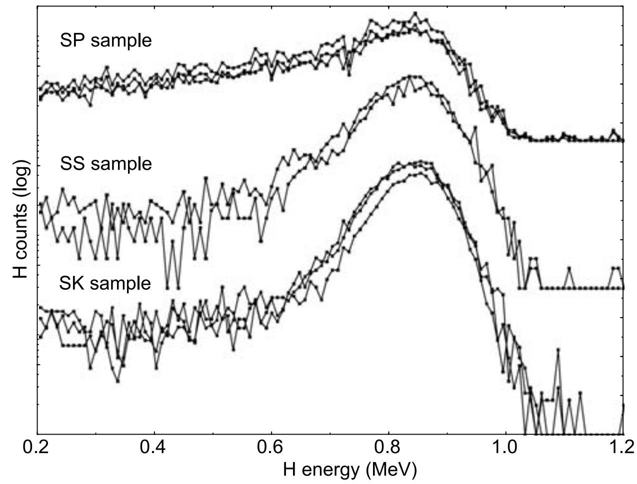

Fig. 4 ERDA spectra for the three samples SS, SP, and SK. Three points have been acquired for sample SP and SK, two for sample SS. Each spectrum presents three specific features: a surface peak, a decay in the 600–800 keV region corresponding to the H diffusion profile, and a plateau regime at low energy attributed to an homogeneous bulk H content

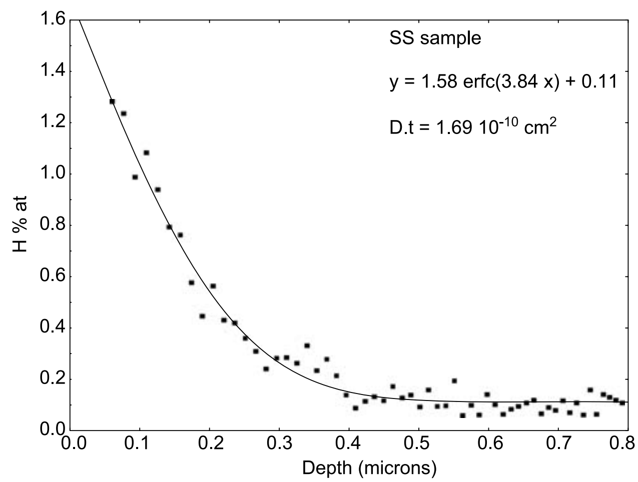

Fig. 5 Diffusion profile derived from the ERDA spectrum for sample SS

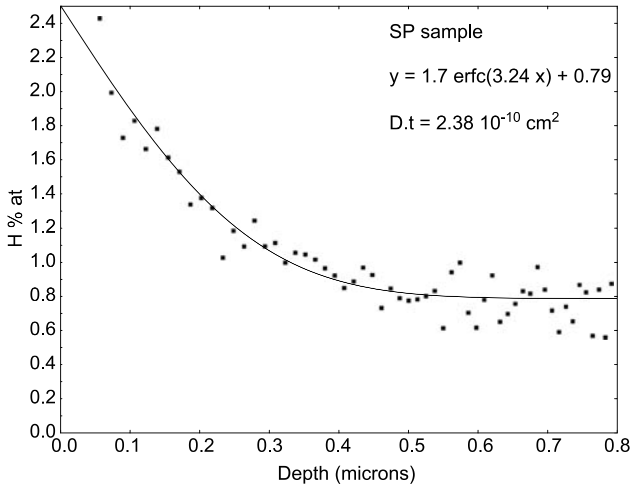

Fig. 6 Diffusion profile derived from the ERDA spectrum for sample SP

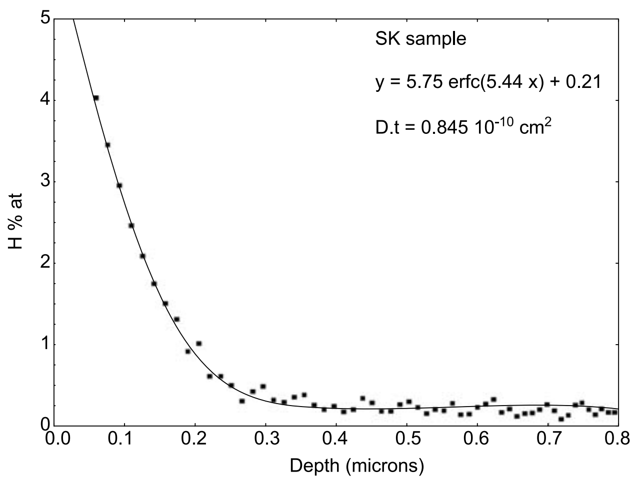

Fig. 7 Diffusion profile derived from the ERDA spectrum for sample SK

Table 1 Values of coefficients of (1) and (3) obtained from three samples SS, SP, and SK derived from ERDA spectra

Sample	α	$H(0,t) - c_i$ at.% H	Dt cm^2	c_i at.% H
SS	75°	1.58	1.69×10^{-10}	0.11
SP	90°	1.70	2.38×10^{-10}	0.79
SK	90°	5.75	0.84×10^{-10}	0.21

the diffusion equation, are comparable to those measured by Ericson and co-workers [17]. Taking into account the age of sample SS ($t_{SS} = 268$ years), its diffusion coefficient is $D_{SS} = 2.0 \times 10^{-20}$ cm^2 s^{-1}, a value coherent with previous measurements obtained for archaeological quartz artifacts.

However all samples, especially SP with 0.79 at.% H, show higher c_i than the values reported in previous work, which may place these measurements out of the model [17]. Several explanations could be considered: (a) the H profile extends so deeply that the plateau regime where c_i is estimated is out of reach in the present experiment, (b) additional H, possibly in form of water inclusions in quartz, could have been accounted for in c_i (Table 1) and may have no influence on hydrogen diffusion, and (c) the poor polishing state of the surface already mentioned in Sect. 2.2 affects the H measurement in grazing geometry by inducing an apparent high H surface content.

The influence of c_i can be interpreted from two opposite points of view. On one hand, if the empirical diffusion coefficient (3) is strictly applied, using $t_{ss} = 268$ years and accounting for the different and high c_i together with the orientations α of all samples, the ages of sample SP and SK can be derived:

$$t_{\text{sample}} = t_{\text{SS}}(D_{\text{sample}} t_{\text{sample}} / D_{\text{SS}} t_{\text{SS}})(c_{i\text{SS}} / c_{i\text{sample}}) \times \exp^{-0.044(\alpha_{\text{SS}} - \alpha_{\text{sample}})},$$

which gives $t_{\text{SK}} = 135$ years (1873 A.D.) and $t_{\text{SP}} = 102$ years (1906 A.D.). We see that although the head SP exhibits the deepest profile, its high c_i strongly reduces its age.

On the other hand, if we consider that the high c_i values indicate that the quartz has reached a saturation level in all samples, then c_i can be regarded as constant, and thus

$$t_{\text{sample}} = t_{\text{SS}}(D_{\text{sample}} t_{\text{sample}} / D_{\text{SS}} t_{\text{SS}}) \exp^{-0.044(\alpha_{\text{SS}} - \alpha_{\text{sample}})},$$

which gives $t_{\text{SK}} = 258$ years (1750 A.D.) and $t_{\text{SP}} = 730$ years (1278 A.D.)

Large uncertainties on the parameters of empirical formula (3) directly affect the results. Moreover, the calculations do not account for the T history of the samples which is unknown. However, both hypotheses lead to the conclusion that sample SK is younger than sample SS dated to 1740 A.D. and that sample SP is possibly older, depending of the model considered. More generally, the dependence of the diffusion penetration on the square root of Dt implies that if two objects exhibit distinct H profiles, as it is the case here, the derived Dt products can be so different that even with large uncertainty on the D coefficient, meaningful results can be deduced about their relative age t. In the present case, the QHD method indicate that the skull SK that has the smallest Dt (Table 1) cannot be of pre-Columbian origin.

4 Conclusions

Examination of the surface of the skull SK and the anthropomorphic head SP by optical and scanning electron microscopy showed distinct features, which were interpreted as fingerprints of manual carving for sample SP and machine lapidary techniques for sample SK. The QHD method has been applied on both samples, by measuring the hydrogen diffusion profile at the surface by ERDA. From the much deeper hydrogen profile exhibited by the head SP relative to the skull SK, it was concluded that the former could be more ancient than the latter. The comparison of the profile of skull SK with that of a reference quartz sample SS dated from 1740 A.D. allowed us to date the manufacture of the quartz skull from the 18–19th century. The two methods used in this work converge and support the conclusion that the anthropomorphic head SP is possibly a genuine pre-Columbian artefact, whereas the rock crystal skull SK has to be considered as a forgery manufactured shortly before its introduction in museum collections in 1878. However further investigations on the QHD method are needed to understand the details of the hydrogen diffusion in natural quartz at room temperature and to improve the confidence in dating rock crystal artefacts. The impact of the various types of defects in quartz, in particular of those introduced by the lapidary techniques on the sample surface properties in connection with water uptake, has to be estimated.

Acknowledgements We wish to thank Mrs. Jane M. Walsh from the Smithsonian Institution in Washington and Mrs. Margaret Sax from the *British Museum* for advices and discussions on surface examination. We are indebted to Y. Adda for the illuminating remarks on the diffusion mechanism of hydrogen in quartz. Many thanks are due to the AGLAE staff, T. Guillou and B. Moignard, for the design and the fabrication of the external beam set-up and L. Pichon for the operation of the data acquisition and to J.J. Ezrati for the operation of the microprofilometer. We are grateful to J.-C. Dran, A. Bouquillon, and M. Menu for their constant and encouraging support. Mrs. K. Klappenbach and the Stiftung Preussische Schlösser und Gärten, Potsdam, Germany, are greatly acknowledged for the loan of the reference quartz sample. Finally, special thanks are due to B. Chantelard and M. Gunn for the logistics and the organization of study of the artefacts of the *Musée du quai Branly*, Paris.

References

1. J. Walsh, Legends of the crystal skulls. Archaeology **61**(3), 36–40 (2008)
2. M. Sax, J.M. Walsh, I.C. Freestone, A.H. Rankin, N.D. Meeks, The origin of two purportedly pre-Columbian Mexican crystal skulls. J. Archaeol. Sci. **35**, 2751–2760 (2008)
3. M.C. Serra, Cristales y obsidiana prehispánicos. Siglo XXI De Mexico Editores (1994)
4. A. Langenscheidt, Los abrasivos en Mesoamérica. Arqueol. Mex. XIV **82**, 55–60 (2006)
5. P. Riviale, Eugène Boban ou les aventures d'un antiquaire au pays des Americanistes. J. Soc. Am. **87**, 351–362 (2001)
6. J. Walsh, Crystal skulls and other problems: or, "don't look it in the eye", in *Exhibiting Dilemmas: Issues of Representation at the Smithsonian*, ed. by A. Henderson, A.L. Kaeppler (Smithsonian Institution Press, Washington, 1997)
7. Reliquary cross with a pierced crystal skull at its base. Private ownership of Mrs. Norma Redo, Mexico.
8. M. Sax, N.D. Meeks, Methods of engraving Mesopotamian quartz cylinders seals. Archaeometry **37**, 25–36 (1995)
9. S.A. Stil, 13858 Aix-en-Provence, France. http://www.stilsa.com
10. T. Laursen, W.A. Lanford, Hydration of obsidian. Nature **276**, 153 (1978)
11. P. Walter, M. Menu, J.-C. Dran, Dating of archaeological flints by fluorine depth profiling: new insights into the mechanism of fluorine uptake. Nucl. Instrum. Methods B **64**, 494 (1992)
12. J.E. Ericson, Anthropology papers, vol. 23 (1982), p. 299
13. Y. Adda, J. Philibert, *La Diffusion dans les Solides* (Presses Universitaires de France, Paris, 1966)
14. O. Dersch, Wasseraufnahme von Quartz: Grundlage für eine Methode zur Datierung archäologischer Quartzartefakte (Water uptake by Quartz: Basis of a method for dating of archaeological quartz artefacts). Doctoral dissertation, J.W. Goethe-Universität Frankfurt am Main, 2001
15. O. Dersch, F. Rauch, Water uptake of quartz investigated by means of ion-beam analysis. Fresenius J. Anal. Chem. **365**, 114 (1999)
16. J. Crank, *The Mathematics of Diffusion*, 2nd edn. (Clarendon Press, Oxford, 1975)
17. J.E. Ericson, O. Dersch, F. Rauch, Quartz hydration dating. J. Archaeol. Sci. **31**, 883 (2004)
18. W.A. Lanford, Analysis for hydrogen by nuclear reaction and energy recoil detection. Nucl. Instrum. Methods B **66**, 65 (1992)
19. Y. Serruys, J. Tirira, P. Trocellier, *Forward Recoil Spectrometry: Applications to Hydrogen Determination in Solids* (Springer, Berlin, 1996)
20. J.C. Dran, J. Salomon, T. Calligaro, P. Walter, Ion beam analysis of art works: 14 years of use in the Louvre. Nucl. Instrum. Methods B **219–220**, 7–15 (2004)
21. T. Calligaro, J. Castaing, J.-C. Dran, B. Moignard, J.-C. Pivin, G.V.R. Prasad, J. Salomon, P. Walter, ERDA with an external helium ion micro-beam, advantages and potential applications. Nucl. Instrum. Methods B **181**, 180 (2001)
22. M. Mayer, SIMNRA, a simulation program for the analysis of NRA, RBS and ERDA, in *Proceedings of the 15th International Conference on the Application of Accelerators in Research and Industry*, ed. by J.L. Duggan, I.L. Morgan. American Institute of Physics Conference Proceedings, vol. 475 (1999), p. 541. http://www.rzg.mpg.de/~mam/AIP%20475-541.pdf
23. J.E.E. Baglin, A.J. Kellock, M.A. Crocket, A.H. Shih, Absolute cross section for hydrogen forward scattering. Nucl. Instrum. Methods B **64**, 469–474 (1992)
24. J.F. Ziegler et al., Profiling hydrogen in materials using ion beams. Nucl. Instrum. Methods **149**, 19–39 (1978)
25. I. Reiche, J. Castaing, T. Calligaro, J. Salomon, M. Aucouturier, U. Reinholz, H.-P. Weise, Analyses of hydrogen in quartz and in sapphire using depth profiling by ERDA at atmospheric pressure: Comparison with resonant NRA and SIMS. Nucl. Instrum. Methods B **249**, 608 (2006)
26. Statistica 7.0, StatSoft, Inc., Tulsa, OK, USA, 2007. www.statsoft.com